Talanta 104 (2013) 75–82

Contents lists available at SciVerse ScienceDirect

Talanta

journal homepage: www.elsevier.com/locate/talanta

Selective determination of gold(III) ion using CuO microsheets as a solid phase adsorbent prior by ICP-OES measurement

Mohammed M. Rahman [a,b,*], Sher Bahadar Khan [a,b], Hadi M. Marwani [a,b], Abdullah M. Asiri [a,b], Khalid A. Alamry [b], Abdulrahman O. Al-Youbi [b]

[a] Center of Excellence for Advanced Materials Research (CEAMR), King Abdulaziz University, Jeddah 21589, P.O. Box 80203, Saudi Arabia
[b] Chemistry Department, Faculty of Science, King Abdulaziz University, P.O. Box 80203, Jeddah 21589, Saudi Arabia

ARTICLE INFO

Article history:
Received 26 September 2012
Received in revised form
9 November 2012
Accepted 12 November 2012
Available online 20 November 2012

Keywords:
CuO microsheets
Wet-chemical process
Adsorption isotherm
Au(III) ion detection
Optical & structural property

ABSTRACT

We have prepared calcined CuO microsheets (MSs) by a wet-chemical process using reducing agents in alkaline medium and characterized by UV/vis., fourier transform infrared (FT-IR) spectroscopy, powder X-ray diffraction (XRD), and field-emission scanning electron microscopy (FESEM) etc. The detailed structural, compositional, and optical characterizations of the MSs were evaluated by XRD pattern, FT-IR, X-ray photoelectron spectroscopy (XPS), and UV–vis spectroscopy, respectively which confirmed that the obtained MSs are well-crystalline CuO and possessed good optical properties. The CuO MSs morphology was investigated by FESEM, which confirmed that the calcined nanomaterials were sheet-shaped and grown in large-quantity. Here, the efficiency of the CuO MS was applied for a selective adsorption of gold(III) ion prior to its detection by inductively coupled plasma-optical emission spectrometry (ICP-OES). The selectivity of CuO MSs towards various metal ions, including Au(III), Cd(II), Co(II), Cr(III), Fe(III), Pd(II), and Zn(II) was analyzed. Based on the adsorption isotherm study, it was confirmed that the selectivity of MSs phase was mostly towards Au(III) ion. The static adsorption capacity for Au(III) was calculated to be 57.0 mg g^{-1}. From Langmuir adsorption isotherm, it was confirmed that the adsorption process was mainly monolayer-adsorption onto a surface containing a finite number of adsorption sites.

1. Introduction

Low-dimensional transition metal oxides have attracted significant attention due to their potential applications in fabricating nano-scale electronics, electro-analytical, selective detection of metal ions, opto-electronics, biological devices, electron field emission sources for emission displays, biochemical detections, and surface enhanced Raman properties etc. [1–4]. Nanostructure materials have attracted a broad-interest due to their exceptional properties and immense potential applications. It exhibits a regular morphological nanostructure, which is composed of a number of regular phases with geometrically-coordinated metals and oxide atoms along the axes. Semiconductor nanostructure materials have concerned significant research effort for its exceptional and outstanding properties as well as versatile applications [5–8]. In last decade, nano-sized transition metal oxides have been extensively studied as promising anodes for Laser-induced-Breakdown-Spectroscopy's since they were first reported by Tarascon et al. [9,10]. Among them, copper oxide (CuO) has attracted much interest owing to its high theoretical capacity, highly-stable, non-toxic, economical approach, and facile synthesis. It is a p-type semiconductor material with a band-gap energy ranging from 1.21 to 1.5 eV [11–13], which is studied for various applications in photo-thermal [14], photo-conductive [15], magnetic [16], and super-conductors devices [17–19] etc. Various efforts have been focused toward the fabrication of nano-structured CuO to improve their performance in currently existing applications. It is also considered as one of the promising artificial mediators due to their properties and functionalities [8,20–24]. Because the electrochemical properties of CuO can be greatly affected by morphologies, intensive research has focused on the controlled synthesis of various CuO nanostructures over the past several years [25–31]. Improved cycling performance has been obtained in most of them. However, it is still a great challenge to achieve high-rate capability and crystallinity in pure CuO nanostructures. It is well accepted that a smaller size of CuO can lead to higher capacity and higher rate capability. This reduces the over potential and allows faster reaction kinetics to detect the metal ions [32–37]. Therefore, the synthesis of CuO nanostructures with ultrafine size is a promising approach to obtain improved large-surface area and high-aspect-ratio in pure CuO nanostructures. Due to the significant properties of semiconductors, the undoped nanomaterials attained a considerable attention in terms of controlled growth of crystalline materials in huge quantity. Various growth techniques

* Corresponding author at: Center of Excellence for Advanced Materials Research and Chemistry Department, Faculty of Science, King Abdulaziz University, Jeddah 21589, P.O. Box 80203, Saudi Arabia. Tel.: +966 59 6421830; fax: +966 26952292.
E-mail address: mmrahman@kau.edu.sa (M.M. Rahman).

0039-9140/$ - see front matter © 2012 Elsevier B.V. All rights reserved.
http://dx.doi.org/10.1016/j.talanta.2012.11.031

have been employed, including the vapor–liquid–solid growth [38], epitaxial-growth [39], vapor–solid growth [40], wet-chemical methods [41], and electro-spinning [42].

In addition, the development of simple, rapid and efficient methods are of interest for monitoring metal ions in the environment. Gold is one of the precious metals and held an allure for thousands of years. It has an exceptional arrangement of properties that have consequence in its exploit in a broad-range of industrial applications. It is also one of nonessential toxic noble elements. Usually, noble metals have received considerable attention due to their widespread applications in fields of petroleum, chemical industry, agriculture, and medicine. Moreover, noble metals can be depicted to the environment by different approaches such as emitting into the atmosphere with automobile exhaust gases. For selective, sensitive, accurate, precise, and interference-free detection of noble metals, a potential separation procedure is generally required prior to the determination of noble metals. Several analytical methods have been applied to analyze metal ions in aqueous solutions, such as atomic absorption spectrometry [43], ICP-OES [44], chelator-modified-gold-electrode [45], SERS [46], anodic stripping voltammetry [47], organosilane-modified electrodes [48], HR-SPR coupled ASV [49], and ion chromatography [50]. However, direct measurements of metal ions, in particular at ultra-trace concentration, by analytical techniques cannot be easily accomplished in aqueous systems because of the lack of sensitivity and selectivity of these methods. Therefore, an efficient extraction procedure is usually required prior to the determination of noble metals for sensitive, accurate, and interference-free determination of noble metals [51]. Several analytical methods can be used for separation of analyte of interest, including liquid–liquid extraction [52], ion exchange [53], co-precipitation [54], cloud point extraction [55], and solid phase extraction (SPE) [56,57]. SPE is considered to be one of the most powerful techniques because it minimizes solvent usage and exposure, disposal costs, and extraction time for sample preparation. Several adsorbents have appeared due to the popularity of SPE for selective extraction of analytes, such as alumina [58], C18 [59], molecular imprinted polymers [60], sensor-array [61], cellulose [62], silica gel [63], activated carbon [64], and carbon nanotubes [65].

The present study was to explore the analytical efficiency of CuO microsheets phase as adsorbent on the selectivity and adsorption capacity of Au(III) prior to its determination by ICP-OES. The selectivity of CuO MSs towards different metal ions, including Au(III), Cd(II), Co(II), Cr(III), Fe(III), Pd(II), and Zn(II), was investigated in order to study the effectiveness of CuO MSs on the adsorption of selected metal ions. Here the calcined undoped CuO microsheets have significant properties such as large-surface area (surface-to-volume ratio) and static adsorption capacity; which offered high adsorbent features that enhanced the direct solid phase adsorption towards the target analytes for the selective detection of Au(III) ions. Based on the selectivity study, it was found that the selectivity of microsheet-phase was the most towards Au(III) ions. The static adsorption capacity for Au(III) was executed in details. Results of adsorption isotherm were also confirmed that the adsorption process was mainly monolayer adsorption onto a surface containing a finite number of adsorption sites. Adsorption data of Au(III) were well fit with the Langmuir classical adsorption isotherm.

2. Experimental sections

2.1. Materials and methods

1000.0 mgL^{-1} stock standard solutions of each Au(III), Cd(II), Co(II), Cr(III), Fe(III), Pd(II), and Zn(II) were purchased from Sigma-Aldrich (Milwaukee, WI, USA). All reagents were used of analytical and spectral purity grade. Doubly distilled de-ionized water was also used throughout experimental studies. Analytical grade of copper chloride and sodium hydroxide was used and purchased from Sigma-Aldrich Company. The λ_{max} (423.0 nm) of calcined CuO microsheets was evaluated with UV/visible spectroscopy (UVO-2960, LABOMED Inc.). FT-IR spectra were performed with a spectrophotometer (Spectrum-100 FT-IR) in the mid-IR range, which was purchased from Bruker, USA. The powder X-ray diffraction (XRD) prototypes were assessed with X-ray diffractometer (Rigaku X-ray difractometer, Mini-Flex 2) equipped with Cu-$K_\alpha 1$ radiation (λ=1.5406 nm) using a generator voltage of 40.0 kV and a generator current of 35.0 mA applied for the purposed. Morphology of undoped CuO MSs was investigated on FE-SEM instrument (FESEM; JSM-7600F, Japan). The XPS measurements were executed on a Thermo Scientific K-Alpha KA1066 spectrometer (Germany). Monochromatic AlKα X-ray radiation sources were used as excitation sources, where beam-spot size was kept in 300.0 μm. The spectra was recorded in the fixed analyzer transmission mode, where pass energy was kept at 200 eV. The scanning of the spectra was performed at pressures less 10^{-8} Torr. ICP-OES measurements were acquired by use of a Perkin Elmer ICP-OES model Optima 4100 DV, USA. The ICP-OES instrument was optimized daily before measurement and operated as recommended by the manufacturers. The ICP-OES spectrometer was used with following parameters: FR power, 1300 kW; frequency, 27.12 MHz; demountable quartz torch, Ar/Ar/Ar; plasma gas (Ar) flow, 15.0 L min^{-1}; auxiliary gas (Ar) flow, 0.2 L min^{-1}; nebulizer gas (Ar) flow, 0.8 L min^{-1}; nebulizer pressure, 2.4 bar; glass spray chamber according to Scott (Ryton), sample pump flow rate, 1.5 mL min^{-1}; integration time, 3.0 s; replicates, 3; wavelength range of monochromator 165.0–460.0 nm. Selected metal ions were measured at wavelengths of 267.60 nm for Au(III), 228.80 nm for Cd(II), 238.90 nm for Co(II), 267.72 nm for Cr(III), 259.94 nm for Fe(III), 340.46 nm for Pd(II), and 206.20 nm for Zn(II).

2.2. Samples preparation and procedure

Stock solutions of Au(III), Cd(II), Co(II), Cr(III), Fe(III), Pd(II), and Zn(II) were prepared in 18.2 MΩ cm distilled de-ionized water and stored in the dark at 4 °C. For selectivity study, standard solutions of 1.0 mg L^{-1} of each metal ion were prepared and adjusted to pH value of 5.0 with acetate buffer. Then, each standard solution was individually mixed with 25.0 mg CuO microsheet materials. In this study, a fixed pH value of 5.0 was chosen for all metal ions in order to avoid any precipitation of other species, in particular for Fe(III). For example, Fe(III) usually gives a precipitation of $Fe(OH)_3$ with buffer solutions at higher pH value than 5.0. For investigation of the static uptake capacity of Au(III), standard solutions of 0, 5.0, 10.0, 15.0, 20.0, 25.0, 30.0, 50.0, 75.0, 125.0, and 150.0 mg L^{-1} were prepared as above, adjusted to the optimum pH value of 5.0 and individually mixed with 25.0 mg CuO microsheets. All mixtures were mechanically shaken for 1.0 h at room temperature.

2.3. Synthesis of CuO microsheets by wet-chemical process

The liquid-phase precipitation was applied to prepare as-grown micro-sheets of CuO by wet-chemical method from $CuCl_2$ as the precipitating agent in basic medium. The starting material ($CuCl_2$) is dissolved in de-ionized water to make 0.1 mol L^{-1} salt solution in round conical flask at room conditions. After addition of NaOH (for adjusting pH at 11.0) into the reactant mixture, it is stirred gradually for 12 h and placed on a hot-plate (at 150.0 °C). The starting materials ($CuCl_2$ and NH_4OH) were used without further purification for precipitation technique. Then the solution was washed with acetone and water

consecutively and kept for drying at room conditions. The as-grown black powders were calcined at 400.0 °C in muffle furnace for 4 h. Finally, the calcined products were characterized in features of their structural, morphological, and optical properties as well as applied for the detection of metal ions uptake.

The development of copper oxide MSs can be well explained based on the chemical reactions concerned and crystal growth behaviors of copper oxides. For the synthesis of CuO MSs, $CuCl_2$ and NaOH were mixed under continuous stirring at 150.0 °C. In reaction system, the NaOH performs a major rule, like control the pH value of the solution as well as resource to supply hydroxyl ions to the solution. The $CuCl_2$ reacts with NaOH and forms $Cu(OH)_2$ upon heating. Further it produced Cu^{+2} and OH^- ions, which consequently assisted in the development of copper oxides according to the chemical reactions:

$$NaOH_{(aq)} \rightarrow Na^{+}_{(aq)} + OH^{-}_{(aq)} \quad \text{(i)}$$

$$CuCl_{2(s)} \rightarrow Cu^{+2}_{(aq)} + 2Cl^{-}_{(aq)} \quad \text{(ii)}$$

$$Cu^{+2}_{(aq)} + 2OH^{-}_{(aq)}\ (pH \sim 11) \rightarrow Cu(OH)_2 \quad \text{(iii)}$$

The $Cu(OH)_2$ finally dissociates (at 150.0 °C) to form of CuO nuclei according to the reaction:

$$Cu(OH)_{2(aq)} \rightarrow CuO_{(s)} + H_2O \quad \text{(iv)}$$

Initially it formed CuO nuclei to perform as building blocks for the development of final products. With reaction time under the appropriate heating conditions in wet-chemical method, the CuO nuclei concentration enlarges which initiates the formation of desired nanomaterial products. As the CuO MSs are prepared by the well growth of low-thickness MSs, therefore it is supposed that the fundamental entity for the configuration of CuO structure is MSs.

3. Results and discussions

3.1. Optical characterization of CuO microshets.

The optical property of the undoped CuO microsheet structure is one of the most important features for the evaluation of its photo-catalytic activity. The optical absorption spectra of MSs are measured by using UV–visible spectrophotometer in the visible range (250.0–800.0 nm). In UV/visible absorption technique, the outer electrons of atoms or molecules are absorbed by incident a radiation source, which undergoes electron transition from lower to higher energy levels. According to the phenomenon, the spectrum is obtained due to the optical absorption, which can be used to analyze the energy band-gap of CuO micromaterials. The optical absorption measurement was carried out at ambient conditions. From the absorption spectrum, an absorbance maximum is measured using calcined CuO MSs at ~423.0 nm, which is presented in Fig. 1(a). Band gap energy (E_{bg}) is calculated on the basis of the maximum absorption band of NCs and found to be 2.9314 eV, according to the following Equation:

$$E_{bg} = \frac{1240}{\lambda}(ev) \quad \text{(v)}$$

where E_{bg} is the band-gap energy and λ_{max} is the wavelength (~423.0 nm) of the microsheets. No extra peak associated with impurities and structural defects were observed in the spectrums, which proved that the synthesized MSs control crystallinity of CuO MSs [66–69].

The undoped CuO MSs were studied in term of atomic and molecular vibrations. FT-IR spectra basically in the region of 400–4000 cm^{-1} are executed at room conditions. Fig. 1(b) displays the FT-IR spectrum of the calcined CuO MSs structures. It represents band at 614 cm^{-1} and 1371 cm^{-1}. These observed wide vibration band (at 614 cm^{-1}) could be assigned as a metal-oxygen (Cu–O) stretching vibration [70], which is demonstrated the configuration of undoped nanostructure materials. The supplementary vibrational bands may be assigned to carbon dioxide molecule vibrations. The absorption bands (1371 cm^{-1}) are exhibited from CO_2, which generally semiconductor nanostructure materials absorb from the environment due to their mesoporous nature [71–74]. At low-frequency region, the vibrational bands are indicated the formation of CuO MSs.

3.2. Morphological, structural, and elemental characterization of CuO microsheets.

High resolution FE-SEM images of calcined CuO microstructures are presented in Fig. 2(b) and (c). The low to high-magnified FE-SEM images of aggregated micro-structural materials are displayed in sheet-shape. Microsheets are composed with nano-dimensional thickness of CuO sheets. The average length of MSs is calculated in the range of 0.62 μm–1.40 μm, which is close to 0.83 ± 10.0 μm. It is clearly exhibited from FE-SEM that the synthesized undoped products are microstructure of CuO. It is revealed in regular sheet-shape with high-density microstructure. The average cross-sectional thickness of sheets is measured from the FESEM image, which is close to $\sim 47.0 \pm 5.0$ nm. It is

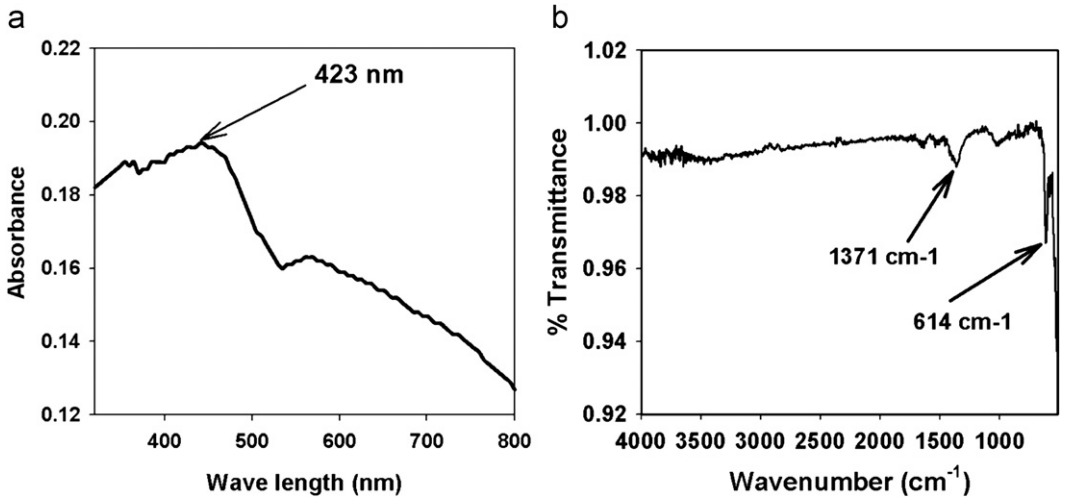

Fig. 1. (a) UV/visible spectroscopy and (b) FT-IR spectroscopy of calcined CuO microsheet materials.

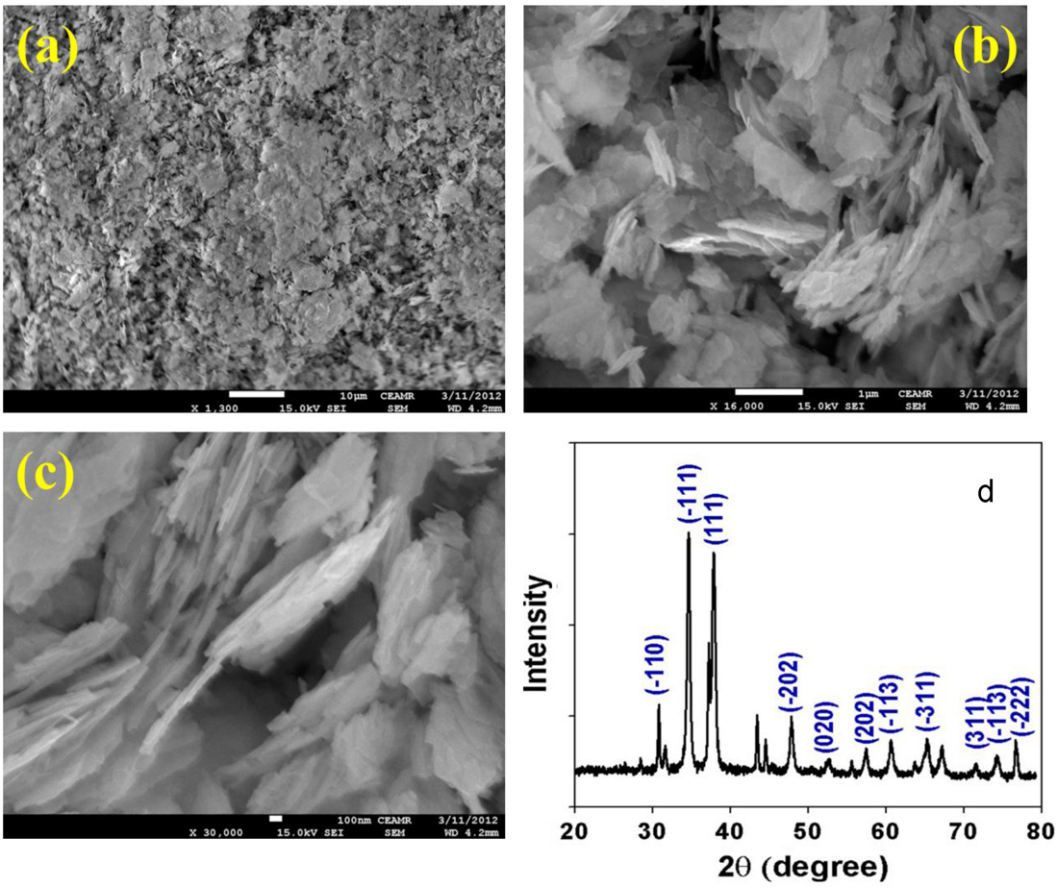

Fig. 2. (a)–(c) Low to high magnified FE-SEM images and (d) powder X-ray diffraction pattern of calcined CuO microsheets.

interesting to note that most of the calcined CuO products are uniformly grown and possessing uniform sheet-shapes. In adding to this, the nano-dimensional sheets are perpendicularly arranged and aligned on the upper-portion of the calcined microsheets. It is also proposed that the wet-chemically prepared micorstructures are composed in sheet-shape of aggregated CuO [75].

To confirm the crystal phases and crystallinity of the calcined CuO microsheets, XRD pattern was employed and presented in Fig. 2(d). The obtained diffraction pattern is well matched with the base centered monoclinic CuO form. According to the JCPDS cards (045–0937), the lattice constants for calcined CuO MSs are found to be a=4.6853 Å, b=3.4257 Å, and c=5.1303 Å. The phases are found the major characteristic peaks (indicated with blue-color) with indices for calcined crystalline SnO_2 at 2θ values of (−1 1 0), (1 1 1), (−1 1 1), (−2 0 2), (0 2 0), (2 0 2), (−1 1 3), (−3 1 1), (3 1 1), (−1 1 3), and (−2 2 2), which are presented in Fig. 2(d). The high-intensity of diffraction peaks in the obtained pattern clearly confirmed that the calcined products are well-crystalline [76]. Except CuO, no other peaks are found in the pattern confirmed that the synthesized microsheets are pure CuO. The crystalline size was also calculated and confirmed using Scherrer formula:

$$D = 0.9\lambda/(\beta\cos\theta) \quad \text{(vi)}$$

where λ is the wavelength of X-ray radiation, β is the full-width at half maximum (FWHM) of the peaks at the diffracting angle θ. The average diameter of CuO MSs is close to ~0.83 μm.

X-ray photoelectron spectroscopy (XPS) is a quantitative spectroscopic technique that measured the elemental-composition, empirical-formula, chemical-state, and electronic-state of the elements that present within a material. XPS spectra are acquired by irradiating a material with a beam of X-rays, while simultaneously determining the kinetic energy and number of electrons that get-away from the top one to ten nm of the material being analyzed. Here, XPS measurements were executed for undoped calcined CuO nanomaterials to investigate the chemical states of CuO. The XPS spectra of Cu2p and O1s are presented in Fig. 3(a). In Fig. 3(b), the spin orbit peaks of the $Cu2p_{(3/2)}$ and $Cu2p_{(1/2)}$ binding energy for all the samples appeared at around 935.2 eV and 956.1 eV respectively, which is in good agreement with the reference data for CuO [77]. The O1s spectrum shows a peak at 531.9 eV in Fig. 3(c). The peak at 531.9 eV is assigned to lattice oxygen, may be indicated to oxygen (i.e., O_2) presence in the undoped CuO nanomaterials [78].

3.3. Detection of Au(III) using selective CuO MSs phase adsorbent (batch method)

3.3.1. Selectivity study of CuO microsheets

Selectivity of the newly prepared CuO MSs phase towards various metal ions was investigated based on determination of the distribution coefficient of MSs Phase. The distribution coefficient (K_d) was calculated [79] from the following Equation:

$$K_d = [(C_o - C_e)/C_e] \times (V/m) \quad \text{(vii)}$$

where C_o and C_e are the initial and final concentrations before and after filtration with CuO MSs, respectively, V refers to the volume (mL) and m is the weight of MSs phase (g). Distribution coefficient values of all metal ions investigated in this study are summarized in Table 1.

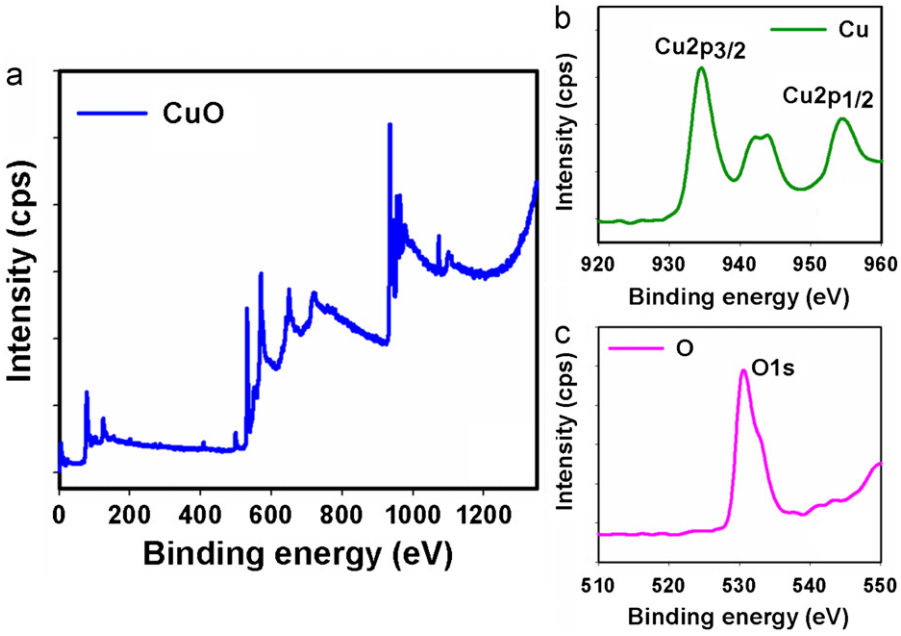

Fig. 3. XPS of (a) Calcined CuO nanomaterials, (b) Cu2p level, and (c) O1s level acquired with MgKα radiation.

Table 1
Selectivity study of CuO microsheets phase adsorption towards different metal ions at pH 5.0 and 25.0 °C ($N=5$).

Metal ions	q_e ($mg\,g^{-1}$)	K_d ($mL\,g^{-1}$)
Au(III)	0.97	36878.79
Zn(II)	0.05	52.63
Cr(III)	0.03	30.93
Co(II)	0.02	20.41
Fe(III)	0.02	20.41
Cd(II)	0.01	10.10
Pd(II)	0.01	10.10

From Table 1, it can be clearly observed that Au(III) has the greatest distribution coefficient value among all metal ions. These results indicated that the selectivity of undoped CuO MS phase towards Au(III) is the most as compared to other metal ions investigated in this study. A schematic representation of Au(III) ion adsorption on the CuO MSs with comparative real FE-SEM images are presented in Fig. 4. In schematic diagram, the FESEM images of MSs are presented before (Fig. 4a) and after (Fig. 4b) adsorption of the gold(III) ion. It is exhibited clearly from the FE-SEM images that the simple wet-chemical methodology of synthesized undoped products are nanostructure of CuO MS, which revealed in aggregated sheet-shape with high-density and high-aspect-ratio. It is also proposed that approximately all of the nanostructure composed in sheet-like shapes of the adsorbed metal ions on the surfaces. Thus, CuO MS phase is capable to selectively bind with Au(III) ions, indicating that the mechanism of adsorption may be electrostatic attraction or physic-sorption or complex formation.

The electron dispersive x-ray spectroscopy (EDS) analysis of these CuO micro-sheets indicates the presence of copper (Cu) and oxygen (O) composition in the pure calcined CuO microstructures before metal ions uptake [Fig. 5(a1)]. It is clearly displayed that the calcined synthesize nanomaterials contained only Cu and O elements, which is presented in Fig. 5(a2). No other peak related with any impurity has been detected in the FESEM coupled EDS, which confirms that the nanostructures are composed only with Cu (68.73%) and O (31.27%), which is revealed in Fig. 5(a3) [area selected from Fig. 5(a1)]. The incorporation of gold ion onto the CuO microstructures via adsorption (ie, physi-sorption or chemi-sorption) method is investigated here. From the EDS observation, it is demonstrated that the gold ions are adsorbed onto the CuO MSs, which is presented in Fig. 5(b1) and (b3).

3.3.2. Static adsorption capacity

For determination of the static adsorption capacity of Au(III) on CuO MS phase, 25.0 mL Au(III) sample solutions with different concentrations (0–150.0 mg L^{-1}) were adjusted to pH 5.0 and individually mixed with 25.0 mg CuO MSs. These mixtures were mechanically shaken for 1.0 h at room temperature. Static adsorption capacity was obtained using the following equation:)

$$q_e = \frac{(C_o - C_e)\ V}{m} \qquad \text{(viii)}$$

where q_e represents the adsorbed Au(III) by the MS phase (mg g^{-1}), C_o and C_e are the initial and equilibrium concentrations of Au(III) ion in solution (mgL^{-1}), respectively, V is the volume (L) and m is the weight of CuO MS phase (g). Fig. 6(a) displays the static uptake capacity of CuO MSs for Au(III) obtained from the experiment of adsorption isotherm. In this study, the adsorption capacity of CuO MSs for Au(III) was found to be 57.0 mg g^{-1}, which is comparable with those previously reported for Au(III) in other studies 12.30 [80], 14.80 [81], 32.00 [82], 33.57 [83] and 72.01[84] mg g^{-1}. The sensitivity (slope) and linearity (R^2) of Au(III) using CuO MSs phase is calculated from the calibration plot (Fig. 6b), which is close to 0.7044 Lg^{-1} and 0.9933 respectively.

3.3.3. Adsorption isotherm models

For developing an equation that accurately represents the results, the analysis of adsorption isotherm data is important. Therefore, a well known model was used to interpret equilibrium isotherm data. The Langmuir Equation is based on an assumption of monolayer adsorption onto a surface containing a finite number of adsorption sites of uniform energies of adsorption with no transmigration of adsorbate in the plane of the surface. The Langmuir adsorption isotherm model is given [85] by the following relation:

$$C_e/q_e = (C_e/Q_o) + 1/Q_o b \qquad \text{(ix)}$$

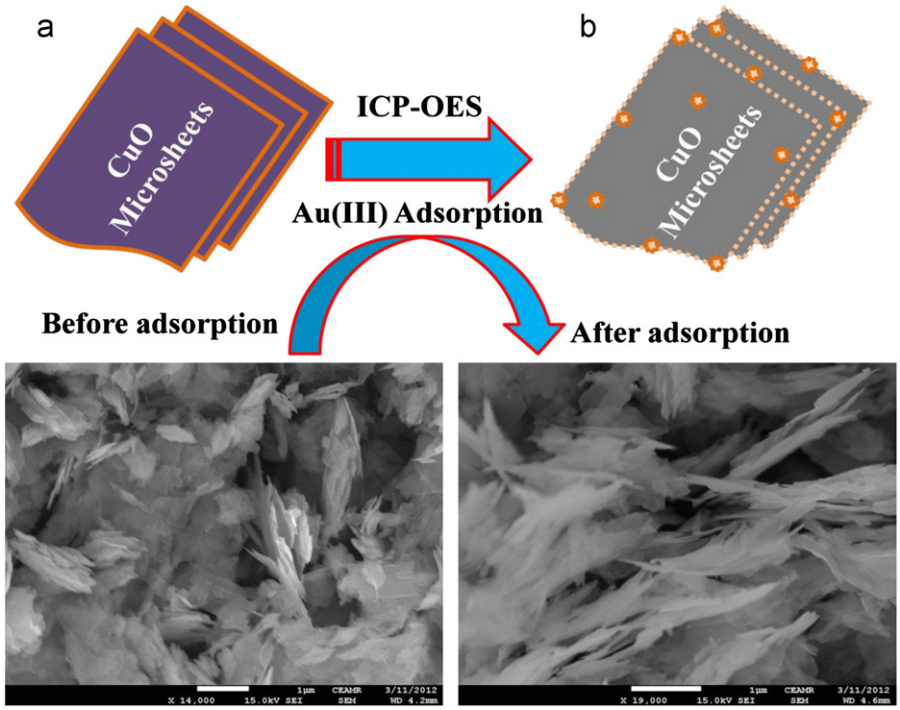

Fig. 4. Schematic representation and FESEM images of (a) before and (b) after Au(III) adsorption on CuO microsheets.

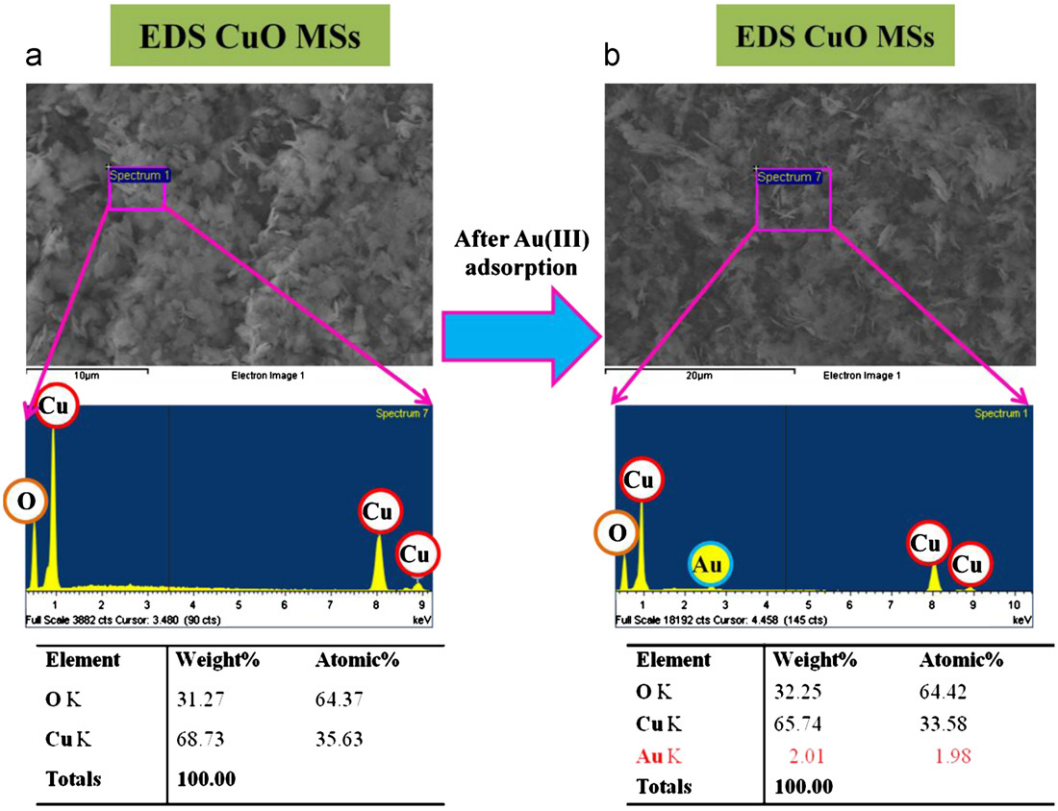

Element	Weight%	Atomic%
O K	31.27	64.37
Cu K	68.73	35.63
Totals	100.00	

Element	Weight%	Atomic%
O K	32.25	64.42
Cu K	65.74	33.58
Au K	2.01	1.98
Totals	100.00	

Fig. 5. EDS investigation of (a) before and (b) after gold(III) adsorption onto calcined CuO microsheets.

where, C_e corresponds to the equilibrium concentrations of Au(III) ion in solution (mg mL^{-1}) and q_e is the adsorbed metal ion by the adsorbate (mg g^{-1}). The symbols Q_o and b refer to Langmuir constants related to adsorption capacity (mg g^{-1}) and energy of adsorption (L mg^{-1}), respectively. These constants can be determined from a linear plot of C_e/q_e against C_e with a slope and intercept equal to $1/Q_o$ and $1/Q_o b$, respectively. Moreover, the essential characteristics of Langmuir adsorption isotherm can be

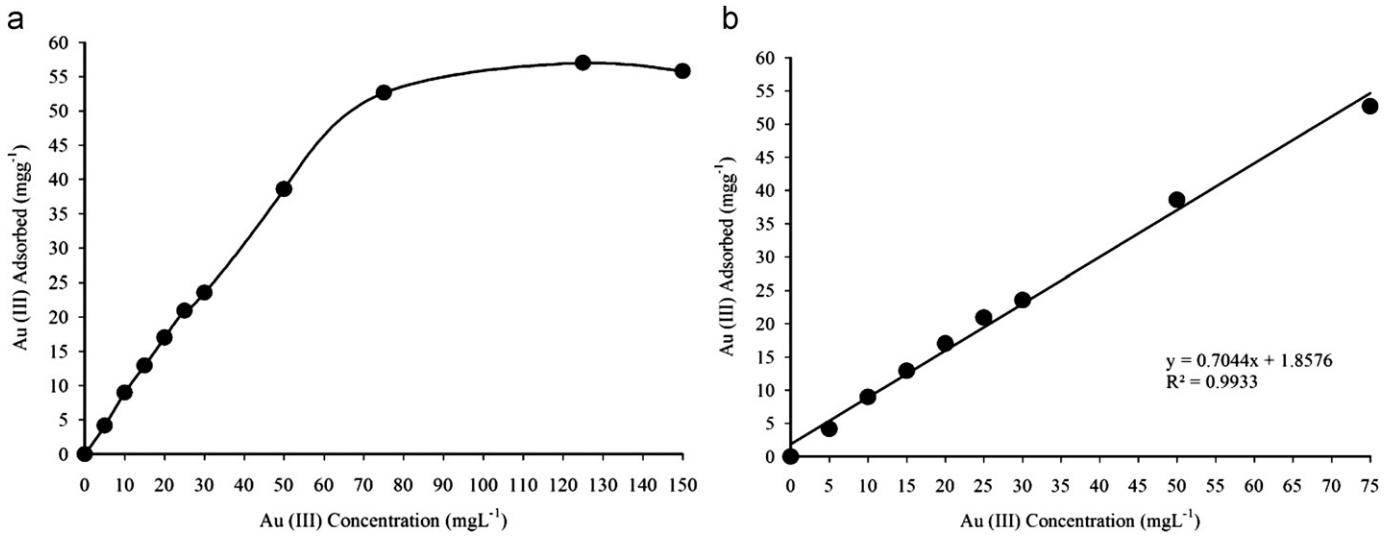

Fig. 6. (a) Adsorption profile and (b) calibration plot of Au(III) on 25.0 mg CuO MSs phase in relation to the concentration at pH 5.0 and 25.0 °C.

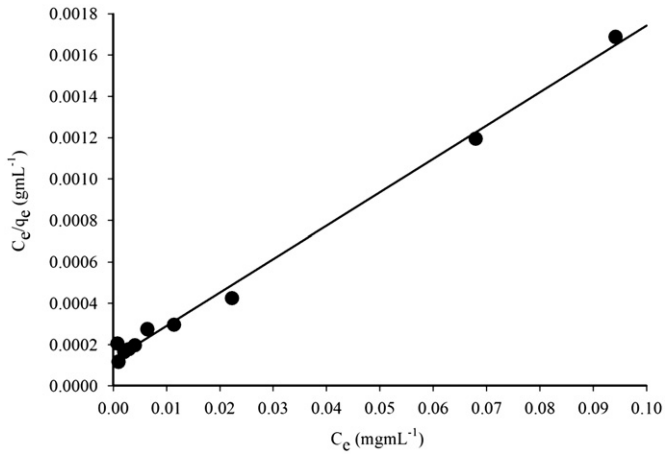

Fig. 7. Langmuir adsorption isotherm model of Au(III) adsorption on 25.0 mg CuO MSs phase at pH 5.0 and 25.0 °C. Adsorption experiments were obtained at different concentrations (0–150.0 mgL^{-1}) of Au(III) under static conditions.

represented in terms of a dimensionless constant separation factor or equilibrium parameter, R_L, which is defined as $R_L = 1/(1+bC_o)$, where b is the Langmuir constant (indicates the nature of adsorption and the shape of the isotherm); C_o the initial concentration of the analyte. The R_L value indicates the type of the isotherm, and R_L values between 0 and 1 represent a favorable adsorption [86].

The experimental isotherm data (Fig. 7) were fit well with the Langmuir equation based on the least square fit, supporting the validity of Langmuir adsorption isotherm model for the adsorption process. Consequently, adsorption isotherm data indicated that the adsorption process was mainly monolayer adsorption onto a surface containing a finite number of adsorption sites. Langmuir constants Q_o and b are found to be 61.93 mg g^{-1} and 0.13 Lmg^{-1}, respectively. The correlation coefficient obtained from the Langmuir model is found to be $R^2 = 0.9950$ for adsorption of Au(III) on CuO MSs. Furthermore, the static adsorption capacity (61.93 mg g^{-1}) calculated from Langmuir equation was in agreement with that (57.0 mg g^{-1}) of the experimental isotherm study. The R_L value of Au(III) adsorption on the CuO MSs is 0.06, supporting a highly favorable adsorption process based on the Langmuir classical adsorption isotherm model.

4. Conclusions

The calcined CuO MSs are successfully prepared by a wet-chemical technique combined with a heat-treatment and characterized in detail in terms of their morphological, structural, and optical properties which displays that the synthesized microstructures possessing monoclinic structure displayed good optical properties. The analytical investigation of the calcined CuO MS phase for selective adsorption and determination of Au(III) in aqueous solution was evaluated. Reasonable static uptake capacity of 57.0 mg g^{-1} with MSs adsorbent for Au(III) in aqueous solution was achieved. Adsorption data of Au(III) were well-fit with the Langmuir adsorption isotherm model. Thus, the method may show considerable promise for using it as an effective approach for a selective separation and determination of Au(III) in complex matrices. The obtained nanosheet composed CuO microstructures is a promising candidate for potential application in metal ions uptake.

Acknowledgments

We would like to thank the Deanship of Scientific Research at King Abdulaziz University for the support of this research via a Research Group Track Grant (No. 3-102/428). Authors are also grateful to Center of Excellence for Advanced Materials (CEAMR) at King Abdulaziz University for providing the research facilities.

References

[1] J. Morales, L. Sanchez, F. Martin, J.R. Ramos-Barrado, M. Sanchez., Electrochim. Acta 49 (2004) 4589.
[2] J.Y. Xiang, J.P. Tu, L. Zhang, Y. Zhou, X.L. Wang, S.J. Shi., J. Power Sources 195 (2010) 313.
[3] M.M. Rahman, S.B. Khan, M. Faisal, A.M. Asiri, K.A. Alamry, Sens. Actuator. B: Chem. 171–172 (2012) 932–937.
[4] M.M. Rahman, S.B. Khan, M. Faisal, A.M. Asiri, M.A. Tariq, Electrochim. Acta 75 (2012) 164–170.
[5] F. Marabelli, G.B. Parravicini, F. Salghetti-Drioli, Phys. Rev. B 52 (1995) 1433.
[6] F.P. Koffyberg, F.A. Benko, J. Appl. Phys. 53 (1982) 1173.
[7] M.M. Rahman, A. Jamal, S.B. Khan, M. Faisal, A.M. Asiri, Microchim. Acta. 178 (2012) 99–106.
[8] M.M. Rahman, A. Jamal, S.B. Khan, M. Faisal, A.M. Asiri, Talanta 95 (2012) 18–24.
[9] F. Wang, W. Tao, M. Zhao, M. Xu, S. Yang, Z. Sun, L. Wang, X. Song, J. Alloy Compd. 509 (2011) 9798.
[10] P. Poizot, S. Laruelle, S. Grugeon, L. Dupont, J.M. Tarascon, Nature 407 (2000) 496.

[11] D. Keyson, D.P. Volanti, L.S. Cavalcante, A.Z. Simoes, J.A. Varela, E. Longo, Mater. Res. Bull. 43 (2008) 771.
[12] V.F. Drobny, D.L. Pulfrey, Thin Solid Film 61 (1979) 89.
[13] A.E. Rakhshani, F.K. Barakat, Mater. Lett. 6 (1987) 37.
[14] A.H. Pfund, Phys. Rev. 7 (1916) 289.
[15] A.E. Rakhshni, Solid State Electron. 29 (1986) 7.
[16] A. Junod, D. Eckert, G. Triscone, J. Muller, W. Reichardt, J. Phys.: Condens. Matter 1 (1989) 8021.
[17] J. Kosa, I. Vajda, J. Mater. Proc. Tech. 181 (2007) 48.
[18] M.M. Rahman, J. Biomed. Nanotech. 7 (2011) 351–357.
[19] M.M. Rahman, A. Umar, K. Sawada, Sens. Actuator: B 137 (2009) 327–333.
[20] Y. Mu, J. Yang, S. Han, H. Hou, Y. Fan, Mater. Lett. 64 (2010) 1287.
[21] L. Chen, C. Zhao, Z. Wei, S. Wang, Y.G.L. Chen, C. Zhao, Z. Wei, S. Wang, Y. Gu, Mater. Lett. 65 (2011) 446.
[22] Q. Pan, H. Jin, H. Wang, G. Yin, Electrochim. Acta 53 (2007) 951.
[23] M. Faisal, S.B. Khan, M.M. Rahman, A. Jamal, A.M. Asiri, M.M. Abdullah, Appl. Surf. Sci. 258 (2012) 7515–7522.
[24] M.M. Rahman, A. Jamal, S.B. Khan, M. Faisal, A.M. Asiri, Chem. Eng. J. 192 (2012) 122–128.
[25] X.P. Gao, J.L. Bao, G.L. Pan, H.Y. Zhu, P.X. Huang, F. Wu, D.Y. Song., J. Phys. Chem. B 108 (2004) 5547.
[26] L.B. Chen, N. Lu, C.M. Xu, H.C. Yu, T.H. Wang, Electrochim. Acta. 54 (2009) 4198.
[27] S.Q. Wang, J.Y. Zhang, C.H. Chen, Scr. Mater. 57 (2007) 337.
[28] S.Q. Wang, J.Y. Zhang, N. Ding, C.H. Chen., Scr. Mater. 60 (2009) 1117.
[29] J.C. Park, J. Kim, H. Kwon, H. Song, Adv. Mater. 21 (2009) 803.
[30] M.M. Rahman, A. Jamal, S.B. Khan, M. Faisal, A.M. Asiri, Sens. Trans. J. 134 (2011) 32–44.
[31] M.M. Rahman, A. Jamal, S.B. Khan, M. Faisal, J. Phys. Chem. C 115 (2011) 9503–9510.
[32] H.B. Wang, Q.M. Pan, H.W. Zhao, G.P. Yin, P.J. Zuo, J. Power Sourc. 167 (2007) 206.
[33] Q.T. Pan, K. Huang, S.B. Ni, F. Yang, S.M. Lin, D.Y. He, J. Alloy Compd. 484 (2009) 322.
[34] M.G. Kim, J. Cho, Adv. Funct. Mater. 19 (2009) 1497.
[35] M.M. Rahman, A. Jamal, S.B. Khan, M. Faisal, Superlatt. Microstruct. 50 (2011) 369–376.
[36] M.M. Rahman, A. Jamal, S.B. Khan, M. Faisal, J. Nanopart. Res. 13 (2011) 3789–3799.
[37] M.M. Rahman, A. Umar, K. Sawada, Adv. Sci. Lett. 2 (2009) 28–34.
[38] R.S. Wagner, W.C. Ellis, Appl. Phys. Lett. 4 (1964) 89.
[39] G.C. Yi, C. Wang, W.I. Park, Semicond. Sci. Technol. 20 (2005) S22.
[40] X. Jiang, T. Herricks, Y.N. Xia, Nano Lett. 2 (2002) 1333.
[41] S. Anandan, X. Wen, S. Yang, Mater. Chem. Phys. 93 (2005) 35.
[42] H. Wu, D. Lin, W. Pan, Appl. Phys. Lett. 89 (2006) 133125.
[43] S.Z. Mohammadi, D. Afzali, D. Pourtalebi, Cent. Eur. J. Chem. 8 (2010) 662.
[44] Y. Li, B. Hu, J. Hazard. Mater. 174 (2010) 534.
[45] T. Stora, R. Hovius, Z. Dienes, M. Pachoud, H. Vogel, Langmuir 13 (1997) 5211.
[46] Y. Wang, J. Irudayaraj, Chem. Commun. 47 (2011) 4394.
[47] Y. Bonfil, E. Kirowa-Eisner, Anal. Chim. Acta. 457 (2002) 285.
[48] Y. Kim, J. Yi, Langmuir 22 (2006) 9805.
[49] S. Wang, E.S. Forzani, N. Tao, Anal. Chem. 79 (2007) 4427.
[50] S. Tanikkul, J. Jakmunee, S. Lapanantnoppakhun, M. Rayanakorn, P. Sooksamiti, R.E. Synovec, G.D. Christian, K. Grudpan, Talanta 64 (2004) 1241.
[51] K. Pyrzynska, Spectrochim. Acta B 60 (2005) 1316.
[52] A. Nasu, S. Yamaguchi, T. Sekine, Anal. Sci. 13 (1997) 903.
[53] G.H. Tao, Z. Fang, J. Anal. Chem. 360 (1998) 156.
[54] M. Soylak, N.D. Erdogan, J. Hazard. Mater. 137 (2006) 1035.
[55] J.L. Manzoori, H. Abdolmohammad-Zadeh, M. Amjadi, Microchim. Acta. 159 (2007) 71.
[56] S.A. Ahmed, J. Hazard. Mater. 156 (2008) 521.
[57] A.M. Alvarez, J.R.E. Alvarez, R.P. Alvarez, J. Radioanal. Nucl. Chem. 273 (2007) 427.
[58] Y.M. Al-Angari, M.W. Kadi, I.M. Ismail, M.A. Gabal, Cent. Eur. J. Chem. 8 (2010) 331.
[59] S. Pei, Z. Fang, Anal. Chim. Acta. 294 (1994) 185.
[60] H.J. Cho, S.W. Myung, Bull. Kor. Chem. Soc. 32 (2011) 489.
[61] M.A. Palacios, Z. Wang, V.A. Montes, G.V. Zyryanov, P. Anzenbacher, J. Am. Chem. Soc. 130 (2008) 10307.
[62] C.G. Rocha-de, A.I. Luiz-de, R.P. dos-Santos, J. Mater. Res. 7 (2004) 329.
[63] Y. Liu, L. Guo, L. Zhu, X. Sun, J. Chen, Chem. Eng. J. 158 (2010) 108.
[64] N.S. Awwad, H.M.H. Gad, M.I. Ahmad, H.F. Aly, Coll. Surf. B 81 (2010) 593.
[65] P. Biparva, M.R. Hadjmohammadi, Clean: Soil Air Water 39 (2011) 1081.
[66] M.M. Rahman, A. Jamal, S.B. Khan, M. Faisal, ACS Appl. Mater. Inter. 3 (2011) 1346.
[67] S.B. Khan, M.M. Rahman, E.S. Jang, K. Akhtar, H. Han, Talanta 84 (2011) 1005–1010.
[68] M. Faisal, S.B. Khan, M.M. Rahman, A. Jamal, A.M. Asiri, M.M. Abdullah, Chem. Eng. J 173 (2011) 178–184.
[69] S.B. Khan, M. Faisal, M.M. Rahman, A. Jamal, Talanta 85 (2011) 943–949.
[70] M.M. Rahman, A. Jamal, S.B. Khan, M. Faisal, Biosens. Bioelectron. 28 (2011) 127.
[71] S.B. Khan, M. Faisal, M.M. Rahman, A. Jamal, Sci. Total Environ. 409 (2011) 2987.
[72] S.B. Khan, K. Akhtar, M.M. Rahman, A.M. Asiri, J. Seo, K.A. Alamry, H. Han, New J. Chem. 36 (2012) 2368–2375.
[73] A. Jamal, M.M. Rahman, S.B. Khan, M. Faisal, K. Akhtar, M.A. Rub, A.M. Asiri, A.O. Al-Youbi, Appl. Surf. Sci. 261 (2012) 52–58.
[74] M. Faisal, S.B. Khan, M.M. Rahman, A. Jamal, A.M. Asiri, M.M. Abdullah, Appl. Surf. Sci. 258 (2011) 672–677.
[75] M. Abaker, S.A. AlSayari, S. Baskoutas, M.M. Rahman, A. AlHajry, S.H. Kim, S.W. Hwang, A. Umar, AIP Conference Proceedings 1370 (2010) 97.
[76] M. Faisal, S.B. Khan, M.M. Rahman, A. Jamal, A. Umar, Mater. Lett. 65 (2011) 1400.
[77] C.C. Chusuei, M.A. Brookshier, D.W. Goodman, Langmuir 15 (1999) 2806–2808.
[78] M.M. Rahman, S.B. Khan, M. Faisal, M.A. Rub, A.O. Al-Youbi, A.M. Asiri, Talanta 99 (2012) 924–931.
[79] D.M. Han, G.Z. Fang, X.P. Yan, J. Chromatogr. A 1100 (2005) 131.
[80] H.B. Senturk, A. Gundogdua, V.N. Bulut, C. Duran, M. Soylak, L. Elci, M. Tufekci, J. Hazard. Mater. 149 (2007) 317.
[81] P. Liang, E. Zhao, Q. Ding, D. Du, Spectrochim. Acta B 63 (2008) 714.
[82] L. Zhang, Z. Li, X. Du, X. Chang, Microchim. Acta 174 (2011) 131.
[83] H.M. Albishri, H.M. Marwani, Arab. J. Chem., http://dx.doi.org/10.1016/j.arabjc.2011.03.017, in press.
[84] H.M. Marwani, H.M. Albishri, T.A. Jalal, E.M. Soliman, Desalin. Water Treat. 45 (2012) 128.
[85] I. Langmuir, J. Am. Chem. Soc. 38 (1916) 2221.
[86] G. Mckay, H.S. Blair, J.R. Gardener, J. Appl. Polym. Sci. 27 (1982) 3043.